Preparation and evaluation of the effect of Fe_3O_4@piroctone olamine magnetic nanoparticles on matrix metalloproteinase-2: A preliminary *in vitro* study

Mojtaba Shakibaie[1]
Mahboobe Haghiri[2]
Mandana Jafari[1]
Sahar Amirpour-Rostami[1]
Alieh Ameri[3]
Hamid Forootanfar[4*]
Mitra Mehrabani[4*]

[1] *Pharmaceutics Research Center, Institute of Neuropharmacology, Kerman University of Medical Sciences, Kerman, Iran*

[2] *The Student Research Committee, Faculty of Pharmacy, Kerman University of Medical Sciences, Kerman, Iran*

[3] *Department of Medicinal Chemistry, Faculty of Pharmacy, Kerman University of Medical Sciences, Kerman, Iran*

[4] *Herbal and Traditional Medicines Research Center, Kerman University of Medical Sciences, Kerman, Iran*

Abstract

In the present study, Fe_3O_4 magnetic nanoparticles were synthesized by the coprecipitation of Fe^{2+} and Fe^{3+} ions and used as a nanocarrier for the production of piroctone-olamine-loaded Fe_3O_4 nanoparticles (Fe_3O_4@PO NPs). The nanocrystalline structure of the prepared iron oxide species was confirmed by the X-ray diffraction spectroscopy method. Particle size distribution analysis showed that the size of Fe_3O_4@PO NPs was in the range of 5–55 nm. The magnetization curve of Fe_3O_4@PO NPs (with saturation magnetization of 28.2 emu/g) confirmed its ferromagnetic property. Loading of PO on the surface of Fe_3O_4 NPs qualitatively verified by Fourier transform infrared spectrum obtained from Fe_3O_4@PO NPs. Cytotoxicity studies on the human fibrosarcoma cell line (HT-1080) revealed higher inhibitory effect of Fe_3O_4@PO NPs (50% cell death [IC_{50}] of 8.1 μg/mL) as compared with Fe_3O_4 NPs (IC_{50} of 117.1 μg/mL) and PO (IC_{50} of 71.2 μg/mL) alone. In the case of human normal fibroblast (Hs68), the viability percentage was found to be 75% in the presence of Fe_3O_4@PO NPs (120 μg/mL). Gelatin zymography showed 17.2% and 34.6% inhibition of matrix metalloproteinase-2 (MMP-2) in the presence of Fe_3O_4@PO and PO, respectively, at the same concentration of 40 μg/mL, whereas Fe_3O_4 NPs did not inhibit MMP-2 at any concentration. Volume 61, Number 6, Pages 676–682, 2014

Keywords: *Fe_3O_4, magnetic nanoparticles, matrix metalloproteinase-2, piroctone olamine, HT-1080*

Abbreviations: *Fe_3O_4@PO NPs, piroctone olamine loaded Fe_3O_4 nanoparticles; FTIR, Fourier-transform infrared; MMP-2, matrix metalloproteinase-2; MNPs, magnetic nanoparticles; TEM, transmission electron microscopy; VSM, vibrating sample magnetometer; XRD, X-ray diffraction.*

**Address for correspondence: Hamid Forootanfar, Pharm D., Ph.D, Herbal and Traditional Medicines Research Center, Kerman University of Medical Sciences, Kerman, Iran. Tel.: +98 341 3205238; Fax: +98 341 3205003; e-mail: h_forootanfar@kmu.ac.ir; Mitra Mehrabani, Pharm D., Ph.D, Herbal and Traditional Medicines Research Center, Kerman University of Medical Sciences, Kerman, Iran. Tel.: +98 341 3205019; Fax: +98 341 3205003; e-mail: mmehrabani@kmu.ac.ir.*

Received 30 August 2013; accepted 2 April 2014

DOI: 10.1002/bab.1231

Published online 18 December 2014 in Wiley Online Library (wileyonlinelibrary.com)

1. Introduction

Special properties of materials at nanoscale compared with corresponding bulk materials encouraged investigators to study the physical, chemical, and biological characteristics of nanostructures synthesized either by physicochemical or biological methods [1]. Among nanomaterials, Fe_3O_4 magnetic nanoparticles (MNPs) received more attention because of the large specific surface area and good superparamagnetic property that allows them to be simply separated by applying a magnetic field [2–4]. The application of Fe_3O_4 MNPs has been well documented in the literature in various areas such as enzyme immobilization [5], magnetic resonance imaging [6], and targeted drug delivery [7]. Recent reports have shown that uptaking of anticancer compounds by tumor cells could be improved after the loading of these agents on the surface of Fe_3O_4 MNPs and applying a magnetic field [8]. Furthermore, in

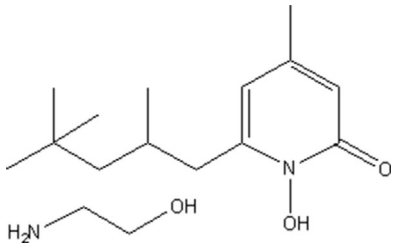

FIG. 1 *The chemical structure of PO.*

some cases, the combination of the various agents with Fe_3O_4 MNPs could improve the therapeutic effect and stability of the produced nanostructures [9, 10].

Matrix metalloproteinases (MMPs) are a major group of enzymes involved in both normal and pathological processes [11, 12]. The key role of these highly homologous, zinc-containing, and calcium-dependent endopeptidases (especially MMP-2 and MMP-9) in cancer development has been well documented in the literature [12]. So, the investigation on compounds with potential inhibitory effect on MMPs activity has been aimed by many studies [12, 13].

Piroctone olamine (PO; Fig. 1), the amino ethanol salt of 1-hydroxy-4-methyl-6-(2,4,4-trimethylpentyl)-2(1H)-pyridone, has been applied in the formulation of cosmetic products, antidandruff shampoos, as well as hair and oral care products [14]. The apoptotic activity of PO on human and murine myeloma and lymphoma cell lines has been recently described by Kim et al. [15]. Furthermore, Fukuda et al. [16] determined the inhibitory effect of PO on the collagenolytic enzyme involved in lesion development in root dentin.

Bearing in mind the above-mentioned points about Fe_3O_4 MNPs and the biological activity of PO, the production and evaluation of the cytotoxic effect of Fe_3O_4 MNPs coated with PO (Fe_3O_4@PO NPs) on the human fibrosarcoma (HT-1080) cell line and the human normal fibroblast (Hs68) were aimed in the present study. In addition, the inhibitory effect of the prepared Fe_3O_4@PO NPs on the activity of MMP-2 secreted by the HT-1080 cell line was also investigated using *in vitro* gelatin zymography.

2. Materials and Methods

2.1. Materials

$FeCl_3 \cdot 6H_2O$, $FeSO_4 \cdot 4H_2O$, sodium hydroxide, and 3-(4,5-dimethylthiazol-2-yl)-2,5-diphenyl-2H-tetrazolium bromide (MTT) were purchased from Merck Chemicals (Darmstadt, Germany). Fetal bovine serum (FBS), Roswell Park Memorial Institute medium (RPMI) 1640, and antibiotics were provided by Gibco / Life Sciences (Gran Island, NY, USA). PO was obtained from Sigma–Aldrich (St. Louis, MO, USA). All other chemicals and solvents were of analytical grade.

2.2. Synthesis of Fe_3O_4 NPs

Fe_3O_4 NPs were synthesized using a modified reported method consisting of the alkalization of aqueous solution containing Fe^{2+} and Fe^{3+} ions in a deoxygenated condition [17]. Briefly, deionized water was boiled for 15 Min and then cooled to room temperature. After deoxygenation of the reaction medium by bubbling nitrogen gas for 1 H, $FeCl_3 \cdot 6H_2O$ (0.48 g) and $FeSO_4 \cdot 4H_2O$ (0.25 g), which was separately dissolved in 100 mL of the deoxygenated deionized water, were mixed by a magnet stirrer (1,000 rpm, 3 Min). Thereafter, 25 mL of sodium hydroxide solution (0.29 M) was dropwise added to the above-mentioned mixture while it was stirred with mechanical agitation at 1,000 rpm. The black precipitate of the Fe_3O_4 NPs appeared at this stage was washed four times with deoxygenated deionized water after 15 Min heating at 80 °C. After separation of the resulting NPs by a magnet, the prepared NPs were lyophilized using a freeze dryer (FD-81; Eyela, Tokyo, Japan) and stored in a sealed container at 4 °C.

2.3. Preparation of Fe_3O_4@PO NPs

To coat PO on the surface of prepared Fe_3O_4 MNPs, the precipitation method given below was used. At first, the chloroform solution of PO (30 mg/mL) was prepared and maintained in a sealed container. Thereafter, Fe_3O_4 NPs suspension was prepared by dispersing 100 mg Fe_3O_4 NPs in deionized water (100 mL) using ultrasonication (100 W, 5 Min). Subsequently, 2 mL of PO solution was added dropwise to the suspension of Fe_3O_4 NPs over a 5 Min period under continuous stirring (300 rpm) using a laboratory magnetic stirrer. The resulting mixture was maintained at 45 °C for 20 Min followed by the separation of PO-coated Fe_3O_4 NPs from the solution by a magnet. Finally, the capped NPs was washed four times with deionized water and lyophilized and stored in a sealed container at 4 °C.

2.4. Characterization of the NPs

The magnetic NPs were characterized using different methods before and after the coating process. For transmission electron microscopy (TEM), one drop of an aqueous suspension containing the NPs, which previously dispersed ultrasonically, was placed on carbon-coated copper TEM grids and dried under an infrared lamp. Micrographs were then obtained using TEM equipment (Zeiss 902A, South Jena, Germany) operated at an accelerating voltage of 80 kV. Particle size distribution patterns of prepared nanostructures were measured by laser light scattering method using a Zetasizer MS2000 (Malvern Instruments, Malvern, UK). X-ray diffraction (XRD) data of the prepared NPs were collected on a P3000 diffractometer instrument (Rich Seifert, NY, USA) employing Cu-Kα radiation at a voltage of 40 kV and a current of 30 mA. The magnetic properties of Fe_3O_4 and Fe_3O_4@PO NPs were determined using a vibrating sample magnetometer (Lakeshore, Westerville, OH, USA, 7307) with a maximum magnetic field of 10 kOe at the room temperature. For qualitative analysis of the coating process, the dried MNPs (before and after the coating process) and PO were used for Fourier transform infrared (FTIR) spectroscopy analysis by

a PerkinElmer (Wellesley, MA, USA) Spectrum One instrument at a resolution of 4 cm^{-1} in KBr pellets.

For quantitative analysis of the coating process, a spectrophotometric method was applied. At first, the standard curve of PO was drawn by plotting the measured absorbance at 304 nm, using a UV–visible spectrophotometer (UVD-2950; Labomed, CA, USA), against different concentrations (2.5–−80 μg/mL) of PO dissolved in ethanol. Thereafter, 200 mg of the washed Fe_3O_4@PO NPs was dispersed and sonicated in ethyl alcohol (50 mL), and absorbances were measured at 304 nm after the separation of the Fe_3O_4 NPs with a magnet. In all absorption measurements, the ethyl alcohol subjected to the same steps with uncoated NPs was applied as the blank. These procedures were performed in triplicate with NPs prepared at different days, and mean of the obtained absorbances was used to measure the amount of the PO coated on the NPs surface.

2.5. Cytotoxicity assay

The HT-1080 cell line and the Hs68 (passages 20–25) were purchased from the National Cell Bank of Iran, Pasteur Institute of Iran (Tehran, Iran). The cells were maintained in RPMI 1640 medium supplemented with FBS (5%), penicillin (100 U/mL), and streptomycin (100 μg/mL) at 37 °C in a CO_2 incubator (5% CO_2 and 95% relative humidity). For cytotoxicity assay, cells (in the exponential phase of growth) were seeded in 96-well tissue culture plates at 2×10^4 cells/well for 24 H. Thereafter, various concentrations (0–120 μg/mL) of PO-coated Fe_3O_4 NPs, Fe_3O_4 NPs, and PO were added to related wells (final volume 200 μL) and incubated for another 24 H. In the case of the HT-1080 cell line, the corresponding supernatants of cultured cells were then collected and assayed for gellatinolytic activity (see Section 2.6). Subsequently, 20 μL of RPMI 1640 medium containing 5 mg/mL of MTT was added to each well and incubated for 3 H followed by replacing the medium by 100 μL of dimethyl sulfoxide and measuring the optical density of the formed purple color at 570 nm. MTT assay was performed in three replicates for each experiment.

2.6. Zymoanalysis

Gelatin zymography was performed according to the method of the previous study [18]. Briefly, aliquots of the treated media (obtained from cultured media of the HT-1080 cell line; see Section 2.5) were loaded onto an SDS-PAGE instrument containing 2 mg/mL gelatin. Electrophoresis was carried out under nonreducing conditions at a constant voltage of 80 V. Thereafter, the gel was gently washed with deionized water (two times) and then one time with Triton X-100 solution (2.5%, v/v) to remove the applied SDS from the gel followed by the incubation of the gel at 37 °C for 48 H in Tris–HCl gelatinase activation buffer (0.1 M, pH 7.4) containing $CaCl_2$ (10 mM). Gel staining was performed with 0.5% Coomassie Brilliant Blue R250 (Sigma), and the proteolysis area of MMP-2 became visible as clear bands against a blue background after intensive destaining. A UVI pro gel documentation system (GDS-8000, Cambridge, UK) was employed for the quantitative evaluation of both the surface and the intensity of the bands, based on the gray levels. Results were compared with nontreated control wells and expressed as the relative expression of MMP-2.

2.7. Statistical analysis

Each value was expressed as the mean ± SD. Software SPSS 15 for windows (SPSS, Chicago, IL, USA) was used for the statistical analysis. Differences between groups were determined using one-way analysis of variance test, and P values of less than 0.05 were considered to be significant.

3. Results and Discussion

3.1. Synthesis and analysis of NPs

Before and after the coating process, the shape and size properties of the synthesized magnetic NPs were studied by TEM. The TEM images of Fe_3O_4 NPs and Fe_3O_4@PO are presented in Figs. 2a and 2b, respectively. The size distribution histograms (Fig. 3) showed that the Fe_3O_4 NPs and Fe_3O_4@PO NPs were in the range between 1–40 and 5–55 nm, respectively.

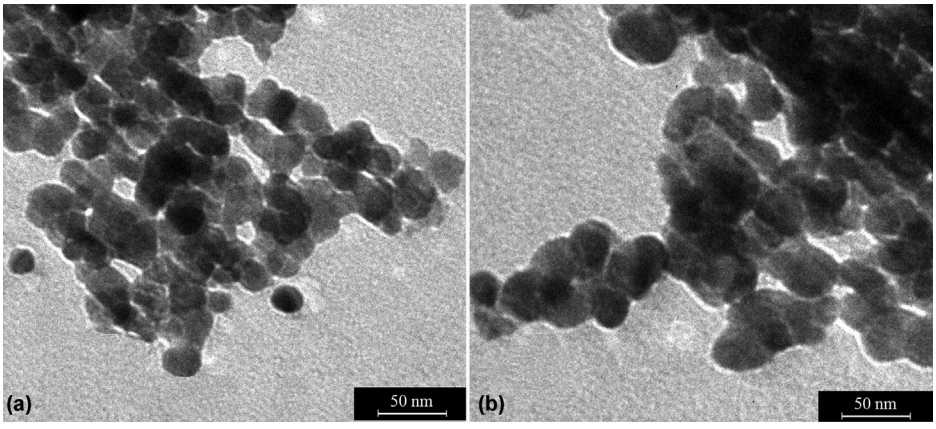

FIG. 2 *TEM micrographs of chemically synthesized (a) Fe_3O_4 NPs and (b) Fe_3O_4@PO NPs.*

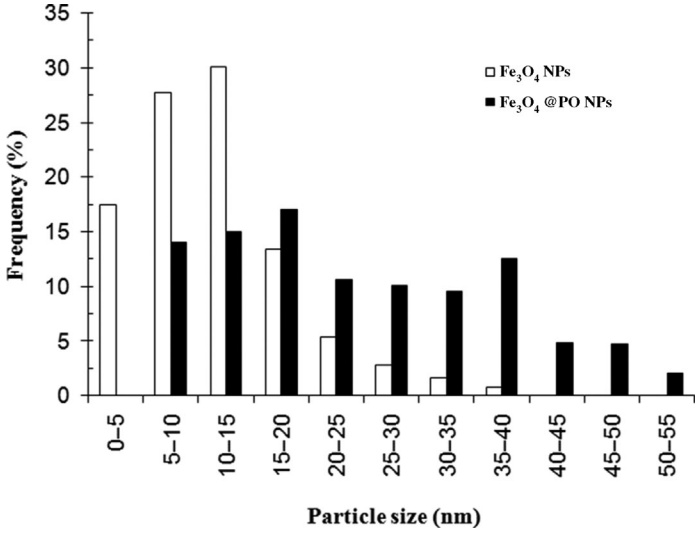

FIG. 3 *The particle size distribution histograms of Fe_3O_4 NPs before and after the coating process with PO.*

Particles with the size of 10–15 and 15–20 nm were the most frequent particles in Fe_3O_4 NPs and Fe_3O_4@PO NPs, respectively (Fig. 3).

Agglomeration between the NPs could be created as a result of large surface area of the NPs and the magnetic forces between NPs [19]. The obtained results showed that the addition of PO on the surface of the magnetic NPs increased the size of related nanoparticles. Such effect was previously reported for the coating of the magnetic NPs with other organic compound such as umbelliprenin [17].

The XRD pattern of Fe_3O_4@PO NPs with seven characteristic peaks of 2θ, 30.1°, 35.6°, 43.3°, 53.5°, 57°, 63°, and 74° (Fig. 4a) confirmed that the magnetic Fe_3O_4@PO were successfully synthesized, and the coating process in the presence of PO did not have an obvious influence on the crystalline structure of Fe_3O_4 MNPs. Same results were determined in the study of Gan et al. [20] where functionalization of Fe_3O_4 MNPs using boronic acid did not affect the XRD pattern of Fe_3O_4 NPs.

The hysteresis curves of Fe_3O_4 MNPs and Fe_3O_4@PO NPs obtained at room temperature (Fig. 4b) show that both samples have an obvious ferromagnetic property. Saturation magnetization (MS) for Fe_3O_4 and Fe_3O_4@PO NPs were found to be 43.7 and 28.2 emu/g, respectively (Fig. 4b), which are obviously lower than that of the bulk Fe_3O_4 (90 emu/g). An increase in the Fe_3O_4 NPs size (as previously described) together with the presence of PO on the surface of MNPs after the coating process might be the probable reason for a decrease in the MS of Fe_3O_4@PO NPs. Same results were reported by Wei et al. [21], indicating that the modification of Fe_3O_4 surface using oleic acid and sodium citrate led to a decrease in the MS.

FTIR measurements were applied to identify the functional groups located on the surface of NPs (Fig. 5). In the present study, the Fe_3O_4 NPs showed the characteristic absorption of Fe–O bond at 632 cm^{-1} (Fig. 5a). However, Fe_3O_4@PO NPs

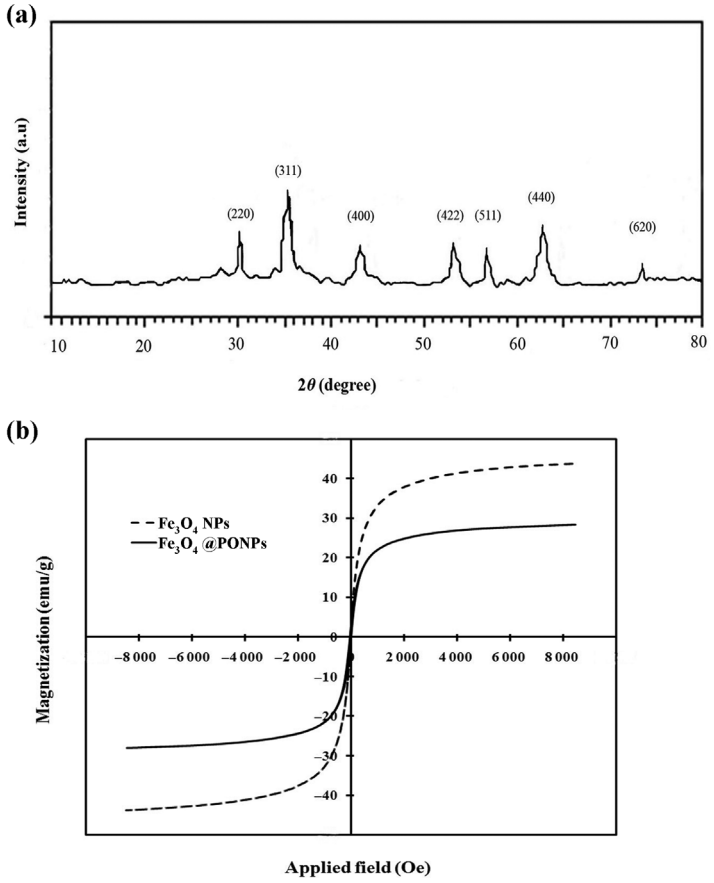

FIG. 4 *(a) X-ray diffraction pattern of Fe_3O_4@PO NPs and (b) magnetic hysteresis curves of Fe_3O_4 NPs and Fe_3O_4@PO NPs obtained at room temperature.*

showed main peaks at 3,000, 1,625, 1,500, 1,366, 1,190, and 627 wave numbers (cm^{-1}) corresponded to O–H or N–H, C=O, C=C, C–N, C–O or C–N, and Fe–O functional groups, respectively (Fig. 5b). The presence of same strong peaks in FTIR spectrum of PO (2,996, 1,622, 1,497, 1,366, and 1,187 cm^{-1}; Fig. 5c) confirmed the success of the coating process. No significant differences were observed between FTIR spectra of the NPs with different synthesis times (data not shown).

A quantitative analysis of the coating process showed that each 1 mg of the coated NPs contained 50 ± 1.3 μg of PO. This amount was determined after washing the NPs by deionized water to remove any unbounded PO. In the study of Khorramizadeh et al. [17] wherein umbelliprenin-coated Fe_3O_4 MNPs were prepared by the same method, it was found that each milligram of coated Fe_3O_4 MNPs contained almost 250 μg of umbelliprenin.

3.2. *In vitro* cytotoxicity study

Cancer cell line

Cytotoxic effects of Fe_3O_4 NPs, Fe_3O_4@PO NPs, and PO alone at different concentrations were evaluated on the HT-1080 cell

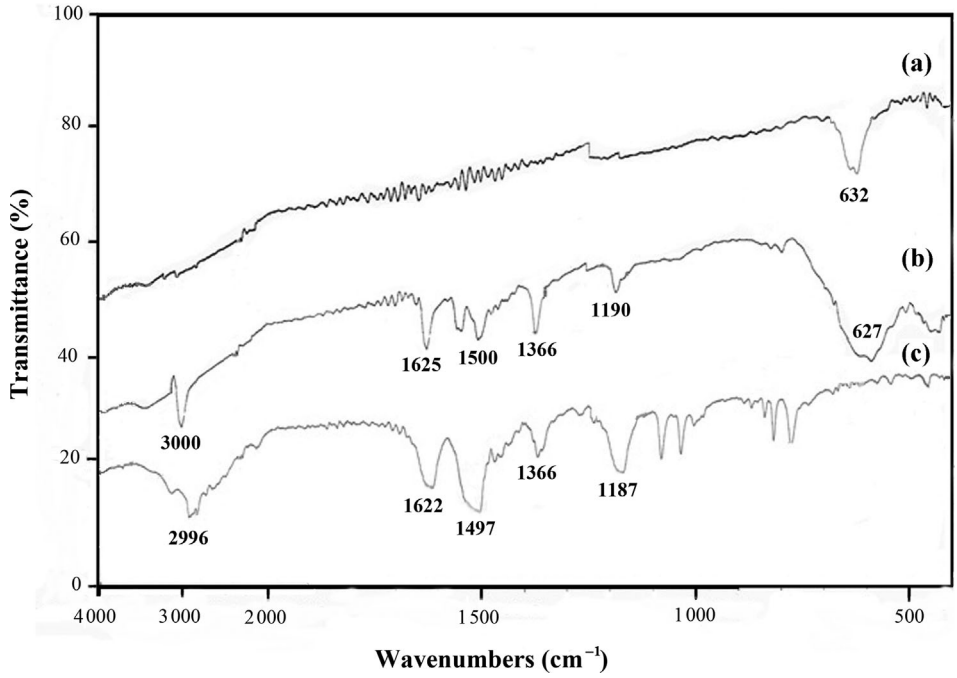

FIG. 5 *FTIR spectrum of (a) Fe_3O_4 NPs, (b) Fe_3O_4@PO NPs, and (c) PO.*

line. Samples were found to have different cytotoxicities on HT-1080 cells in a direct dose–response relationship pattern, with the Fe_3O_4@PO being the most potent one (Fig. 6a). For all concentrations, the cytotoxic effect of the Fe_3O_4@PO NPs is significantly higher than Fe_3O_4 NPs and PO ($P < 0.05$). Moreover, the required concentrations to cause 50% cell death (IC_{50}) were 117.1 and 71.2 μg/mL in cells treated with Fe_3O_4 and PO, respectively. Fe_3O_4@PO NPs created the same effect (*i.e.*, 50% cell death) at a very low concentration of 8.1 μg/mL. In other words, the new combination of PO and Fe_3O_4 NPs was significantly more potent than each compound alone ($P < 0.05$).

Behind the antidandruff activity of PO, the ability of this antifungal agent for the inhibition of myeloma cell lines via the inhibition of Wnt/beta catenin signaling pathway has been determined by Kim et al. [15]. The IC_{50} of PO on myeloma (U-266, RPMI 8226, and KMS18) and lymphoma (LAM-53 and Raji) cell lines was found to be 179 μg/mL [15]. Obtained results of the present study revealed IC_{50} of 71.2 μg/mL for PO on the HT-1080 cell line. Literature review showed a significant difference in biological activities of cytotoxic agents and its Fe_3O_4 MNPs-conjugated form in both *in vitro* and *in vivo* models. In other words, lower amounts of cytotoxic compounds will be needed to produce the same antiproliferative effect when cytotoxic agents loaded on Fe_3O_4 MNPs [17]. So, the efficiency of PO in conjugation with Fe_3O_4 MNPs to inhibit the HT-1080 cell line was also investigated in the present study. The obtained results showed that the cytotoxic activity of PO (IC_{50} of 71.2 μg/mL) was increased when coated on the surface of Fe_3O_4 MNPs (IC_{50} of 8.1 μg/mL) (Fig. 6a). Same results was reported by Khorramizadeh et al. [17] who indicated an IC_{50} of 9 μg/mL for umbelliprenin-coated Fe_3O_4 MNPs compared with umbelliprenin (a bioactive sesquiterpene coumarin) alone, which showed IC_{50} of 50 μg/mL. They ascribed such an observation for the improvement of water solubility of target compounds after loading on Fe_3O_4 MNPs [17]. A better penetration of Fe_3O_4@PO NPs toward cell membrane together with solubility improvement of PO might be the possible reason for lower IC_{50} of Fe_3O_4@PO NPs on the HT-1080 cell line achieved in our study.

Normal cell line

The Hs68 cell was applied to determine the cytotoxic effect of the prepared nanostructure on normal cells. Compared with the cancer cell line (HT-1080), all applied compounds (Fe_3O_4 NPs, Fe_3O_4@PO NPs, and PO alone) represented lower toxicity on the Hs68 cell (Fig. 6b). At the highest concentration of Fe_3O_4@PO NPs (120 μg/mL), the viability of the Hs68 cell was found to be 75%, whereas Fe_3O_4 MNPs exhibited viability of 89% at the same concentration (Fig. 6b). The obtained results of the toxicity evaluation of Fe_3O_4 MNPs toward normal cells have been found to be variable. For example, in the study of Cheng et al. [19], Fe_3O_4 MNPs did not show any toxic effect on Cos-7 cells (monkey kidney cells). Same results were reported by Shundo et al. [22], indicating the 100% survival of mouse embryonic stem cells after the exposure to Fe_3O_4 MNPs at high concentration of 750 μg/mL. The obtained results of Hua et al. [23] revealed that the prepared carrier (poly-[aniline-co-N-(1-one-butyric acid) aniline] (SPAnH) coated on Fe_3O_4 cores)

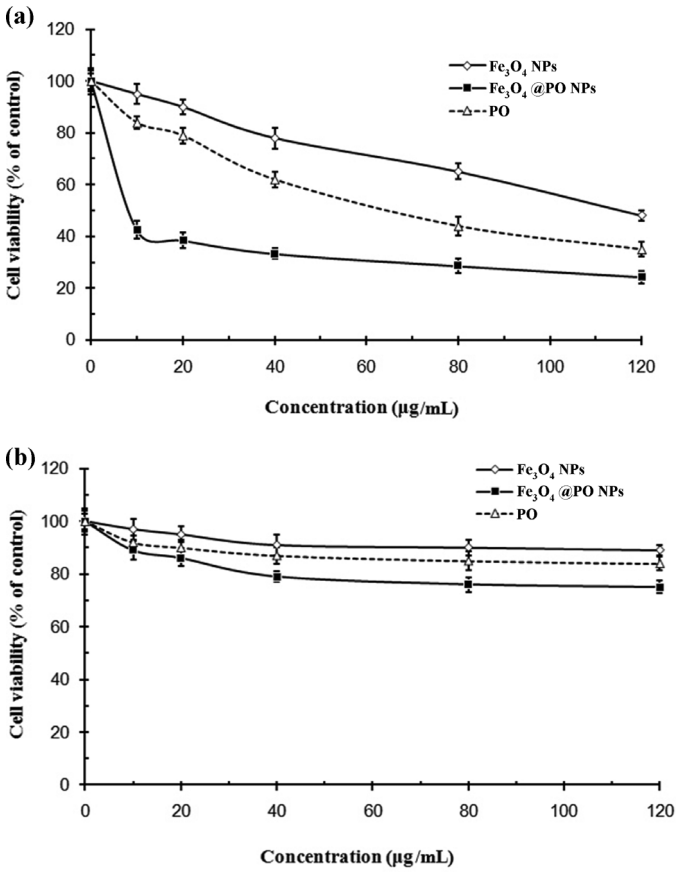

FIG. 6 *The cytotoxic effect of Fe_3O_4 NPs, Fe_3O_4@PO NPs, and PO on (a) HT-1080 cell line and (b) Hs68 cell. Data are presented as mean ± SD.*

applied for the immobilization of carmustine (a chemotherapeutic agent used for the treatment of malignant brain tumors) represented no cytotoxic effect on human umbilical vein endothelial cells after 48 H incubation. However, the applied fibroblast in the investigation conducted by Berry et al. [24] was found to be completely inhibited by Fe_3O_4 MNPs.

3.3. Zymographic studies

MMPs form a family of more than 20 zinc-dependent proteinases involved in the remodeling of extracellular matrix. They are believed to play a critical role in various disease states such as cancer, inflammation, and degenerative diseases [25]. A strong association between the activity of MMPs, especially MMP-2 (Gelatinase A) and MMP-9 (Gelatinase B), and an invasive phenotype in several tumors had been well documented. So, the screening of MMP inhibitors (even small molecules or peptides) as therapeutic agents in various tumors has been targeted by many investigators [25]. Fibrosarcoma cell lines (*e.g.*, WEHI 164 and HT-1080) are one of the most common cell models applied for the *in vitro* study of MMP-2 and MMP-9 activity [26–28]. So, in the present study, the inhibitory effects of the Fe_3O_4 NPs, Fe_3O_4@PO NPs, and PO on MMP-2 activity secreted by the HT-1080 cell line were also

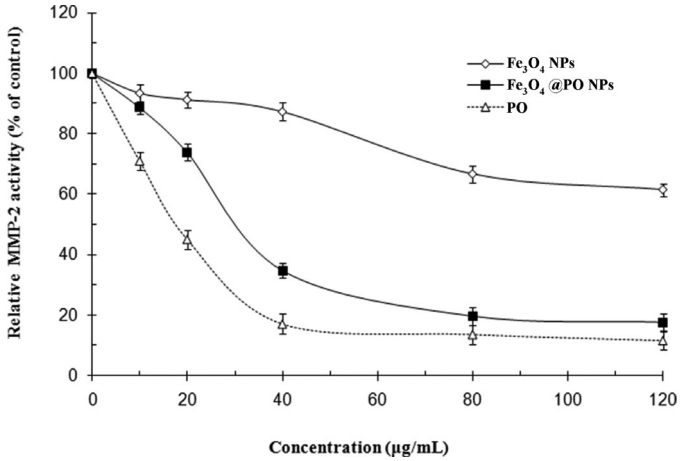

FIG. 7 *MMP-2-inhibitory effect of Fe_3O_4 NPs, Fe_3O_4@PO NPs, and PO on HT-1080 fibrosarcoma cell line.*

examined. As illustrated in Fig. 7, the relative activity of MMP-2 in the presence of Fe_3O_4@PO NPs and PO (at a concentration of 40 µg/mL) decreased to 34.6% and 17.2%, respectively, whereas only 12.8% of an initial activity of MMP-2 reduced after the treatment of the HT-1080 cell line by the same concentration of Fe_3O_4 NPs. Most of the investigated MMP inhibitors contain zinc binding groups (ZBGs) such as hydroxamic acid in their structures, which strongly interacts with the zinc ion in the catalytic site of an MMP [25, 29]. Such ZBGs is present in the structure of PO (Fig. 1) and might be the possible reason for the inhibitory activity of PO in the present investigation. Furthermore, this probable mechanism justifies the lower MMP-2-inhibitory activity of Fe_3O_4@PO NPs compared with free PO (Fig. 7) because the accessibility of bond PO in Fe_3O_4@PO NPs for interacting with ZBGs of MMP-2 was decreased.

4. Conclusions

In the present work, PO was coated on the surface of Fe_3O_4 MNPs synthesized by the alkalization of an aqueous medium containing Fe^{2+} and Fe^{3+} ions, and its cytotoxic effect on the HT-1080 cell line and Hs68 was evaluated. To sum up, the obtained results of the cytotoxic investigation revealed that in spite of Fe_3O_4@PO NPs potency to inhibit the HT-1080 cell line, PO-loaded MNPs showed lower cytotoxicity toward normal fibroblast cells. These results suggested that Fe_3O_4@PO NPs possess a great selectivity between cancer and normal cells. The MMP-2 inhibitory effect of Fe_3O_4@PO NPs (studied by gelatin zymographic) was found to be lower than PO alone.

5. Acknowledgements

This work was supported financially by grant number 91/251 from the Pharmaceutics Research Center, Kerman University of Medical Sciences (Kerman, Iran). We also thank the

Iranian Nanotechnology Initiative Council for its admirable participation in this study.

6. References

[1] Shi, J., Votruba, A. R., Farokhzad, O. C., and Langer, R. (2010) Nano Lett. 10, 3223–3230.
[2] He, Q., Wu, Z., and Huang, C. (2012) J. Nanosci. Nanotechnol. 12, 2943–2954.
[3] Lu, A. H., Salabas, E. L., and Schüth, F. (2007) Angew. Chem. Int. Ed. 46, 1222–1244.
[4] Wei, Y., Yin, G., Ma, C., Huang, Z., Chen, X., Liao, X., Yao, Y., and Yin, H. (2013) Colloids Surf. B 107, 180–188.
[5] Liu, X., Chen, X., Li, Y., Cui, Y., Zhu, H., and Zhu, W. (2012) J. Nanopart. Res. 14, 1–7.
[6] Zhu, X., Zhou, J., Chen, M., Shi, M., Feng, W., and Li, F. (2012) Biomaterials 33, 4618–4627.
[7] Veiseh, O., Gunn, J. W., and Zhang, M. (2010) Adv. Drug Deliv. Rev. 62, 284–304.
[8] Wang, X., Zhang, R., Wu, C., Dai, Y., Song, M., Gutmann, S., Gao, F., Lv, G., Li, J., and Li, X. (2007) J. Biomed. Mater. Res. A 80, 852–860.
[9] Si, H. Y., Li, D. P., Wang, T. M., Zhang, H. L., Ren, F. Y., Xu, Z. G., and Zhao, Y. Y. (2010) J. Nanosci. Nanotechnol. 10, 2325–2331.
[10] Zhang, Q., Wang, C., Qiao, L., Yan, H., and Liu, K. (2009) J. Mater. Chem. 19, 8393–8402.
[11] Bjorklund, M., and Koivunen, E. (2005) Biochim. Biophys. Acta 1755, 37–69.
[12] Murphy, G., and Nagase, H. (2008) Mol. Aspects Med. 29, 290–308.
[13] Mook, O. R. F., Frederiks, W. M., and Van Noorden, C. J. F. (2004) Biochim. Biophys. Acta Rev. Cancer 1705, 69–89.
[14] Schmidt-Rose, T., Braren, S., Fölster, H., Hillemann, T., Oltrogge, B., Philipp, P., Weets, G., and Fey, S. (2011) Int. J. Cosmetic Sci. 33, 276–282.
[15] Kim, Y., Alpmann, P., Blaum-Feder, S., Kramer, S., Endo, T., Lu, D., Carson, D., and Schmidt-Wolf, I. G. H. (2011) In Vivo 25, 99–103.
[16] Fukuda, Y., Nakashima, S., and Ujiie, T. (2009) Am. J. Dent. 22, 115–121.
[17] Khorramizadeh, M. R., Esmail-Nazari, Z., Zarei-Ghaane, Z., Shakibaie, M., Mollazadeh-Moghaddam, K., Iranshahi, M., and Shahverdi, A. R. (2010) Mater. Sci. Eng. C 30, 1038–1042.
[18] Shakibaie, M., Khorramizadeh, M. R., Faramarzi, M. A., Sabzevari, O., and Shahverdi, A. R. (2010) Biotechnol. Appl. Biochem. 56, 7–15.
[19] Cheng, F. Y., Su, C. H., Yang, Y. S., Yeh, C. S., Tsai, C. Y., Wu, C. L., Wu, M. T., and Shieh, D. B. (2005) Biomaterials 26, 729–738.
[20] Gan, Q., Lu, X., Yuan, Y., Qian, J., Zhou, H., Lu, X., Shi, J., and Liu, C. (2011) Biomaterials 32, 1932–1942.
[21] Wei, Y., Han, B., Hu, X., Lin, Y., Wang, X., and Deng, X. (2012) Procedia Eng. 27, 632–637.
[22] Shundo, C., Zhang, H., Nakanishi, T., and Osaka, T. (2012) Colloids Surf. B 97, 221–225.
[23] Hua, M.-Y., Liu, H.-L., Yang, H.-W., Chen, P.-Y., Tsai, R.-Y., Huang, C.-Y., Tseng, I.-C., Lyu, L.-A., Ma, C.-C., Tang, H.-J., Yen, T.-C., and Wei, K.-C. (2011) Biomaterials 32, 516–527.
[24] Berry, C. C., Wells, S., Charles, S., and Curtis, A. S. G. (2003) Biomaterials 24, 4551–4557.
[25] Hu, J., Van den Steen, P. E., Sang, Q.-X. A., and Opdenakker, G. (2007) Nat. Rev. Drug Discov. 6, 480–496.
[26] Ma, X., and Chan, E. C. Y. (2010) J. Chromatogr. B 878, 1777–1783.
[27] Wan, R., Mo, Y., Zhang, X., Chien, S., Tollerud, D. J., and Zhang, Q. (2008) Toxicol. Appl. Pharmacol. 233, 276–285.
[28] Wang, T., Zhang, Y., Wang, Y., and Yue-hu Pei, Y.-H. (2007) Toxicol. In Vitro 21, 646–650.
[29] Nicolotti, O., Catto, M., Giangreco, I., Barletta, M., Leonetti, F., Stefanachi, A., Pisani, L., Cellamare, S., Tortorella, P., Loiodice, F., and Carotti, A. (2012) Eur. J. Med. Chem. 58, 368–376.